marine ecology
an evolutionary perspective

Marine Ecology. ISSN 0173-9565

SPECIAL TOPIC

Temperature variability and algal isotopic heterogeneity on a Floridian coral reef

Malcolm D. Stokes[1], James J. Leichter[2], Stephen Wing[3] and Russell Frew[3]

1 Marine Physical Laboratory, Scripps Institution of Oceanography, La Jolla, CA, USA
2 Scripps Institution of Oceanography, La Jolla, CA, USA
3 Department of Marine Science, University of Otago, Dunedin, New Zealand

Keywords
Coral; ecosystems; reef; stable isotope.

Correspondence
Malcolm D. Stokes, Scripps Institution of Oceanography, Marine Physical Laboratory, 8820 Shellback Way, La Jolla, CA, USA, 92037-0238.
E-mail: dstokes@ucsd.edu

Accepted: 6 June 2011

doi:10.1111/j.1439-0485.2011.00469.x

Abstract

On Conch Reef, Florida Keys, USA, we examine relationships between temperature variability measured with a unique, high-resolution sensor network, and the abundance of benthic reef organisms and carbon, nitrogen and oxygen stable isotopic composition of two abundant macroalgal species. Visualization of spatial temperature anomalies mapped onto measured reef bathymetry reveals episodic thermal patchiness and persistent thermal features likely indicating meter scale variability in nutrient supply. These patterns result from the relatively shallow depths of the offshore thermocline and an active internal wave field creating a hydrographic structure conducive to interactions of an offshore, subthermocline nutrient pool with reef topography. The distribution of major benthic reef organism taxa, as well as the stable isotopic composition of C, N and O, from the macroalgae *Dictyota menstrualis* and *Halimeda tuna* are all highly variable on scales of less than 10 m and are not necessarily depth-dependent. Covariability between spatial patterns of the temperature minima, depth and $\delta^{13}C$ of *D. menstrualis* and *H. tuna* suggest a role of oceanographic forcing in inorganic carbon acquisition in these species. Comparisons of the measured temperature with the predicted temperature based on $\delta^{18}O$ from *H. tuna* aragonite suggest a possible influence of low salinity water in the system and non-linear interactions between ambient conditions and calcification at fine temporal and spatial scales. These observations have implications for the interpretation of both contemporary and paleontologic reef environments where oceanographic forcing interacts with complex reef topography.

Introduction

Coral reefs form one of the most biologically diverse and productive marine ecosystems. These dynamic communities develop as a complex mosaic of primary and secondary producers, microbes, sessile benthic as well as mobile demersal and planktonic organisms, all of which are heterogeneously distributed in both space and time. Perhaps more so than in any other marine ecosystem, key functional guilds of the biota – particularly the corals themselves – function as 'foundation species', or 'ecosystem engineers' (*sensu* Dayton 1985) and produce the physical structure critical for the development of the complex ecosystem. The bank-barrier reefs along the south coast of Florida and the Florida Keys, like reefs in many locations, exhibit scales of spatial patchiness in the distribution of primary substrate and benthic organisms that vary from the scale of centimeters between individuals to many kilometers of separation between the shoals, islands and cays along the length of the Florida Keys Reef Tract (FLKRT). Interactions between the physical heterogeneity of structure built by the foundation species and the dynamic

oceanography in this region result in a rich and heterogeneous physical and biological environment across a large range of scales. This study examines spatial patterns of species distributions and stable isotopic composition in relation to thermal fluctuations associated with reef topography at small (meter to tens of meter) scales.

Variation in the water masses to which a reef is exposed can strongly influence thermal and salinity conditions, nutrient dynamics, fluxes of suspended particles and dissolved organic and inorganic carbon, as well as water column light attenuation influencing benthic primary production. One approach to simplifying the understanding biological responses to the complex suite of physical drivers is to sample the spatial and temporal patterns in tissue chemistry of sessile organisms that integrate signals of resource availability through time. The stable isotope composition of marine organisms can provide useful information regarding integrated chemical and physical environmental conditions, providing the various biologically driven discrimination processes associated with uptake and integration of environmental signals are understood. Observations of tissue carbon isotopic composition in primary producers can provide insight into the sources of inorganic carbon supporting primary productivity and taxon-specific carbon fixation pathways (*e.g.* Raven *et al.* 1982; Kübler & Raven 1994; Cornelisen *et al.* 2007; Hepburn *et al.* 2011). Analysis of nitrogen stable isotopes has served as a means of identifying nutrient sources and transformation pathways in a variety of marine ecosystems. For example, δ^{15}N values of biological materials within nitrogen cycles reflect both the isotopic signatures of nitrogen sources and biological discrimination associated with uptake and biogeochemical transformation (Altabet 2001). If differential nutrient sources have distinct isotopic compositions, it can be possible to trace their uptake by primary producers (*e.g.* Umezawa *et al.* 2002; Cole *et al.* 2005; Leichter *et al.* 2007) and cycling in consumer food webs (*e.g.* Fourqurean *et al.* 1997; McClelland & Valiela 1998; Cole *et al.* 2005). In the Florida Keys, Leichter *et al.* (2003, 2007) observed patterns of increasing δ^{15}N in a benthic macroalga with increasing exposure to subthermocline water masses containing nitrate with high δ^{15}N relative to the expected signature of inshore, and shallow water potential nitrogen sources. In addition to providing insight into nutrient sources, analysis of δ^{15}N values of organic matter in marine ecosystems can also reveal decomposition processes (Saino & Hattori 1980) and trophic dynamics (Hansson *et al.* 1997). Stable isotopic composition in marine sediments can also provide insight into broadscale ecosystem function in both the past and the present (Altabet 2005). Analysis of other stable isotopes, particularly of oxygen (δ^{18}O) from marine sediments and from calcifying marine organisms, can reveal chemical and physical attributes of the environment when the calcification occurred. Analysis of δ^{18}O from long-lived and well preserved calcifying organisms, particularly when coupled with information on elemental ratios such as barium:calcium and strontium:calcium, have been widely used to reconstruct paleo-ocean temperature time series (*e.g.* Grossman & Ku 1986), to infer past variation in ocean salinity (Ren *et al.* 2002) and to provide natal origin markers in marine organisms with pelagic larvae (*e.g.* Tabouret *et al.* 2010).

Closely coupled to the biological and biochemical processes that mediate any reef ecosystem are the physical variables of the environment (*i.e.* light intensity, temperature, water motion, *etc.*) that vary on many different spatial and temporal scales. Thus, in studying community structure and ecosystem function it is valuable, and at times essential, to understand natural sources of variability over biologically relevant spatial and temporal scales of meters to tens of meters and minutes to hours. Along the FLKRT, episodic but widespread variation in temperature and input of nutrients is caused by upward excursions of the local thermocline associated with frontal eddies of the Florida Current (Lee & Mayer 1977; Lee *et al.* 1985) and with the impact of turbulent internal bores arriving at tidal and faster frequencies (Leichter *et al.* 1996, 2003, 2005). Prior research has shown enhanced growth rates of both benthic algae and suspension feeding corals associated with enhanced fluxes of nutrients and suspended particles with internal waves (Leichter *et al.* 1998, 2003; Smith *et al.* 2004), and enhanced heterotrophic grazing on phytoplankton over more rugose reef terrain with high current velocities (Monismith *et al.* 2010). Rapid temperature variability associated with internal waves on reefs can also be important *per se* because of physiological stresses in corals occurring at both high and low temperature (Brown 1997; Knowlton & Jackson 2001).

Because coral reefs characteristically develop in highly oligotrophic waters, high biological affinity for available nutrients and tight recycling are key attributes of system-level biogeochemical cycling. However, as in all ecosystems, net new primary production is also dependent on sources of inorganic nutrients, primarily nitrogen and phosphorus. Inorganic N and P can arrive from myriad sources, including *in situ* fixation, fluxes out of reef matrices and sediments, terrestrial surface and groundwater runoff, atmospheric deposition, and localized upwelling of nutrient-rich subsurface waters (reviewed in D'Elia & Wiebe 1990). Recent evidence also suggests nitrification by microbial communities hosted within benthic sponges may be a significant source of nitrate on shallow Florida reefs (Southwell *et al.* 2008). The potential limitation of nutrient uptake in corals and other

sessile primary producers by boundary layer transport processes (*e.g.* Atkinson & Bilger 1992) further implies strong physical mediation of overall nutrient availability, particularly in shallow water and in oceanic settings, where reefs are exposed to open ocean waves and currents. Closer to shore, and especially near islands such as in the Florida Keys, major sources of inorganic nutrients are likely to include terrestrial inputs, associated with rainfall and runoff transporting nitrate, nitrite, ammonium, and phosphate into the marine environment (*e.g.* Umezawa *et al.* 2002). Primary production in the Florida Keys marine environment is, therefore, likely supported by multiple distinct but at times overlapping major sources of nutrients: oceanic inputs associated with high frequency upwelling events for the offshore reef tract and adjoining offshore environments, contrasting with largely terrestrial sources transported primarily by surface and submarine runoff for nearshore environments (see Kruczynski & McManus 2002). At least for the outer reef slopes, the association between nutrient concentrations and temperature fluctuations implies that temperature time series, which are relatively easy to measure, can serve as useful indicators of nutrient variation, which is much more difficult to sample.

In the present study we explore relationships between high frequency environmental variability measured across a densely sampled spatial grid and patterns of whole community composition and of $\delta^{13}C$, $\delta^{15}N$, and $\delta^{18}O$ of two primary producers on a Florida coral reef. The unique level of spatial resolution allows us to examine variation across depths as well as to map the more subtle variation within isobaths expressed as depth-specific thermal anomalies. The gross similarity between maps of different physical and biological parameters is quantified and we then construct a series of linear models to test for statistically significant relationships between a suite of temperature metrics (and, by proxy, offshore nutrient input) and the biological data and use an information theoretic approach to rank the explanatory power of the various statistical models (Burnham & Anderson 2002). This approach allows us to ask whether depth and various aspects of the measured thermal environment are, or are not, related to both the community composition and the tissue isotopic composition at the spatial scale of the individual sampling nodes across the study area. Previous work on ^{13}C, ^{15}N and ^{18}O isotopic variability in macroalgal tissues suggests correlations along reef depth gradients; however, previous research tends to have only limited spatial sampling along isobaths. Our approach, utilizing a densely sampled spatial grid allows us to ask explicitly how the physical environment, benthic community and macroalgal tissue chemistry vary both across and within depths, and which environmental variables best predict the observed biological patterns. For *Halimeda tuna* carbonate material we are then also able to explore the differences between observed temperature and temperatures predicted on the basis of $\delta^{18}O$ values and steady state assumptions about $\delta^{18}O$ of the ambient seawater. The high degree of spatial variance in measured *H. tuna* $\delta^{18}O$ suggests potential roles of salinity variation as well as possible non-linear responses of calcification to temperature fluctuations.

Methods

We deployed a unique, high-resolution sensor system, the Benthic Oceanographic Array (BOA; Deane & Stokes 2002), to measure temperature variability on the reef surface over an area of approximately 12,000 m^2 (a grid approximately 80 × 150 m) during a period of high thermal variability (Leichter *et al.* 2005). Concomitantly, and at the same spatial resolution, we measured the abundance of major benthic taxa across the study area and collected tissue samples of two species of abundant macroalgae for analysis of C, N and O isotopic composition. These observations are visualized as spatial maps of the temperature and biological data across the entire sampling grid.

Study area

The data for this study were collected at Conch Reef in the Florida Keys (24°57.0′ N, 80°27.3′ W) (Fig. 1), a site of long-term coral reef research on the Florida Keys reef tract and the location of the Aquarius Habitat undersea laboratory operated by the National Undersea Research Center (NURC) of the National Oceanic and Atmospheric Administration (NOAA). This location is similar to other reefs in the upper Florida Keys, consisting of a Holocene veneer of scleractinian corals, hydrozoans, sponges, coralline and filamentous and fleshy algae encrusting the Plio-Pleistocene carbonate platform. The reef crest at 8–10 m depth and the fore reef both slope gradually (*c.* 2–5% slope) to a step at approximately 16 m depth where the slope becomes steeper (*c.* 8–15% slope) down to the base of the reef at 30–32 m depth. A series of parallel, low (1–2 m height) coral spurs separated by sand channels, transect the fore reef slope. At the base of the fore reef, a gradually sloping (1–5%) sand plain extends seaward of the reef approximately 20–30 km to the deeper channel of the Straits of Florida. Alongshore currents at Conch Reef are typically 0.1–0.5 ms^{-1} flowing towards the northeast with tidal reversals to the southwest. Offshore of the reef site (1–5 km) the flows are stronger (0.5–2.0 ms^{-1}) and driven by the Florida Current primarily towards the northeast. The surface tides at Conch Reef are mixed semidiurnal with a mean amplitude of approximately 0.5–0.75 m.

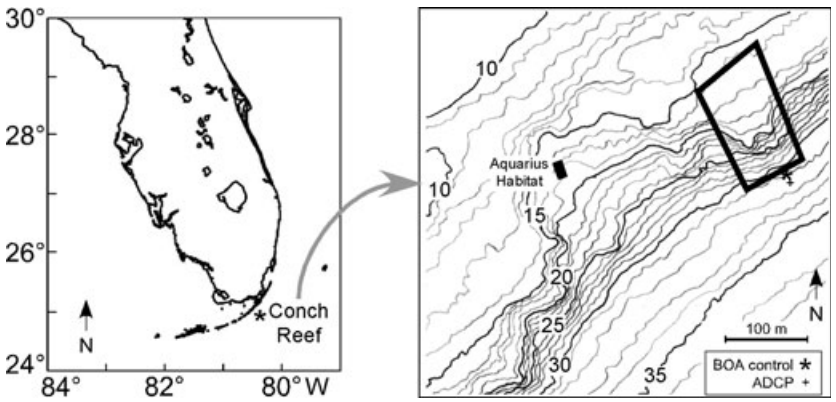

Fig. 1. Map of the study site at Conch Reef (24°57.0′ N, 80°27.3′ W) near the southern tip of Florida, USA. Bathymetric contours (in 1-m intervals), the Aquarius Habitat, the location of the deployed array (black outline), BOA control and ADCP locations are indicated on the right.

Details of the fine-scale physical oceanography of the Conch Reef site can be found in Leichter *et al.* (2005), who deployed a dense array of instruments spatially overlapping this study site in 2003 as well as during 2004 (and on a less dense spatial scale almost continuously since 1992; see Leichter *et al.* 2003, 2007). Our studies have shown that during approximately half the year, May through September, the water column and benthic boundary of Conch Reef is strongly influenced by the episodic incursion of cool, sub-thermocline water from offshore of the reef slope, driven by strong semidiurnal internal tides and higher frequency internal wave activity (see also Davis *et al.* 2008). The advected water masses interact with the reef bathymetry, producing a heterogeneous temperature and nutrient environment both across the reef bathymetry (depths) and within isobaths. In addition, there are areas with persistent warm and cool temperature anomalies associated with the reef topography. The cool water intrusions are characterized by onshore current flow and elevated levels of nutrients and plankton densities, up to an order of magnitude higher than background levels, and temperature fluctuations as great as 8 °C. Incursion events can penetrate into shallow water (<10 m depth) beyond the reef crest and can last anywhere from 20 min to several hours. The pooling of cool, dense water constrained within pockets and depressions of low relief can be evident for up to several hours following individual incursion events. During the winter months, the water column can be 6–8º cooler than the summer maximum temperatures and the offshore mixed-layer extends to deeper depths. Occasional atmospheric cold fronts can cause surface temperatures to drop below 20 °C for periods of up to several days. Associated with the breakdown of stratification in approximately October through January, the subsurface thermal variability due to internal waves is reduced. The thermal structure and current flow patterns impacting Conch Reef are compounded by the localized seasonal variability in stratification that modulates high-frequency variation associated with internal waves, changes in the volume transport of the Florida Current (Niiler 1968) and the propagation of Florida Current spin-off eddies (Lee & Mayer 1977; Lee *et al.* 1985).

Instrumentation

The instrumentation was deployed from June through September 2004, and systematic benthic sampling and surveying of the study site was conducted at the beginning of that time period during an Aquarius Habitat saturation diving mission (10–23 June). During the high frequency component of the study, the primary technology used was an extensive temperature sensor array capable of synchronized, high precision, autonomous sampling for extended periods, known as BOA (Benthic Oceanographic Array, Deane & Stokes 2002). The system consisted of 100 temperature sensors arranged in 10 arrays of 10 elements spaced serially along cables at 15-m intervals. The BOA system allows synchronous sampling of all sensors at a 5-s interval with a resolution and accuracy of 0.007° and 0.04 °C, respectively. Sensor nodes were anchored to the reef by fixing them to a 25-cm spike driven into the bottom or tied onto dead coral outcroppings. The 10 array cables were connected to a submersible junction box at the BOA control and power supply located at the base of the reef slope at approximately 33 m depth, adjacent to an acoustic Doppler current profiler (ADCP; RDI Workhorse 600 kHz) with pressure sensor. The ADCP sampled at 1.33 Hz and stored 1-min averages in 1-m vertical bins. Detailed ADCP data are presented (Leichter *et al.* 2005). Individual temperature recorders (Seabird Electronics SBE39, 0.002 °C accuracy sampling at 10-s intervals) were also deployed immediately adjacent to the BOA nodes at the deepest and shallowest corners of the array. One BOA strand was fixed to a vertical mooring near the BOA

junction box to provide water column temperature measurements in approximately 2.5- m intervals between 30 and 3 m depth.

In addition to the high-frequency sampling described above, benthic temperature was measured continuously throughout 2004 at 10, 20, and 30 m depth adjacent to this BOA reef site with SBE39 temperature recorders (0.001 °C resolution). Data were sampled at 2-min intervals and averaged in 10-min bins for the yearly dataset.

Once the BOA sensor nodes were in place, the array was mapped *in situ*. The survey was conducted on two length scales. A large-scale mapping was made of the BOA grid and reef topology using compass board, calibrated measuring tape, and digital depth gauge (see Fig. 2). This procedure located the node positions within <0.5 m in horizontal space and to within approximately 0.3 m in depth. The node locations were surveyed relative to fixed markers on the sea floor (*i.e.* permanent moorings for the Aquarius habitat of known GPS position). Four 1.0-m^2 photographic quadrats were sampled near each node location using a housed digital Nikon camera mounted on a frame to quantify the percent coverage of benthic invertebrates (here grouped as hermatypic corals, turf and macroalgae, and epilithic sponges) as well as to identify the substrate type and any small-scale fluctuations in topography on the order of cm around the sample locations.

BOA data analysis

The detailed principles and algorithms used to analyze the sensor array data and the error estimates for the calculated temperature anomalies, can be found in Deane & Stokes (2002) and for Conch Reef, FL, in Leichter *et al.* (2005). For every time step in the data record, the mean profile of temperature as a function of depth is calculated with a 3-m vertical averaging length scale. Subtracting this mean profile from the raw data record yields a within-depth, horizontal temperature anomaly. Because the thermal field at Conch Reef during the summer months is dominated by vertical gradients, isolating this temperature component allows a detailed examination of the smaller, time-varying component contained in a temperature anomaly and indicative of horizontal gradients across the reef slope. Spatial and temporal variation in the anomaly arises from a number of factors including the nature of the cool water incursions on the reef, driven by internal waves, and their interaction with the reef bathymetry. Any within-depth heterogeneity of temperature along isobaths results in nonzero values of the temperature anomaly. To visualize the extensive dataset, values of the temperature and temperature anomaly and other sampled metrics from all BOA nodes were interpolated as color contour surfaces on a 4-m grid and mapped onto the measured reef bathymetry.

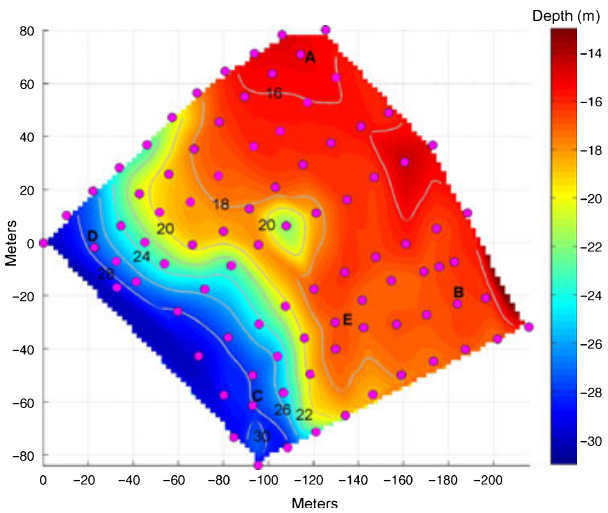

Fig. 2. Detailed bathymetry and sensor node locations at the study site. Sensor locations are indicated by the circles. The depths of selected contour intervals are indicated by the numerals. Nodes in the quadrants at points A–E are referenced in the text.

Isotopic sampling

Samples of *Halimeda tuna* and *Dictyota menstrualis* were collected where present, from each node position of the array, rinsed in de-ionized water, and then dried and prepared for isotopic analysis. *Halimeda tuna* samples were divided into two equal parts, half treated with 0.1% HCl to remove calcium carbonate and half treated with 0.1% NaOH to remove the organic component. These samples were then ground into a fine powder with mortar and pestle and weighed subsamples were placed in tin capsules for isotopic analysis.

For each of the samples of macroalgae tissue, subsamples of 1–5 mg were analyzed for $\delta^{13}C$ and $\delta^{15}N$ at IsoTrace NZ Ltd. (Dunedin, New Zealand) on a Europa 20–20 update stable isotope mass spectrometer (MS; Europa Scientific, Crewe, UK) interfaced to a Carlo Erba elemental analyzer (NA1500; Carlo Erba, Milan, Italy) in continuous flow mode (precision: 0.2‰). Analysis was calibrated to EDTA laboratory standard reference (Elemental Microanalysis, Cheshire, UK) and standardized against international standards (IAEACH-6 for carbon, IAEAN1 and IAEAN2 for nitrogen). Results are expressed in standard delta notation where, for example, $\delta^{13}C = [(Rsample/Rstd)-1]*1000$ where Rsample = $^{13}C/^{12}C$ and Rstd = $^{13}C/^{12}C$ of Peedee belemnite limestone and atmospheric N_2.

Samples of calcium carbonate from *H. tuna* were independently analyzed for $\delta^{18}O$ and $\delta^{13}C$. Aliquots

(2–3 mg) of ground samples were reacted with 103% H_3PO_4 under vacuum overnight. Carbon dioxide produced by this reaction was purified and analyzed on a Thermo Finnigan mass spectrometer for carbon and oxygen ratios. The same procedure was followed for NBS (National Bureau of Standards) 18 and NBS 19 carbonate standards. Results are reported in the standard delta (δ) notation against the standard mean ocean water (SMOW).

Statistical analyses

To investigate the statistical relationships between community composition as well as C:N and isotopic variability (δ^{13}C, δ^{15}N of *Dictyota menstrualis;* δ^{13}C, δ^{15}N, δ^{18}O of *Halimeda tuna*) with our high resolution measurements of environmental variables (depth (m), mean, minimum, maximum and variability in temperature) we constructed a series of distance-based linear models (DISTLM; Anderson *et al.* 2008). We then used a permutational model to select the best fit models based on Akaike's information criterion (corrected for inclusion of multiple explanatory variables) AICc (Burnham & Anderson 2002; Anderson *et al.* 2008). Marginal tests based on a permutational ANOVA platform provide a measure of fit for each relationship.

There is a growing suite of techniques for quantitatively comparing spatial maps of key environmental variables and for describing spatial patterns and heterogeneity (see Rose *et al.* 2009). The task of quantifying similarity between two-dimensional maps is complex and the application of the techniques is itself the subject of lengthy discourse beyond the scope of this investigation. Therefore, the techniques used here are only briefly summarized below and the full details can be found in the appropriate geospatial analysis literature (*e.g.* Monseurd & Leemans 1992; Pontius 2000; Hagen 2003; Hagen-Zanker 2006).

To perform similarity comparisons between the spatial maps of various metrics, the original data maps (*i.e.* Figs 4–7) were first rasterized into an equivalent 100×100 cell grid and the data within each grid normalized such that each cell value was between 0 and 1. All computations were performed using MATLAB™ and the Riks Map Comparison Tool Kit (Visser & De Nijs 2006).

Indices describing the spatial organization of the maps were calculated following Hagen-Zanker (2006). This includes the two-dimensional Shannon entropy index of diversity, which provides a measure of the composition of the map based on the proportional contents of the individual map cells. Higher entropy values of the index indicate a more varied map composition. The fractal dimension of the map was calculated, which characterizes the complexity of the spatial structure present in the map based on the size and shape of individual map patches. The calculated fractal dimension varies between 1 (simple shapes) and 2 (patches of higher convolution).

The Shannon entropy index was calculated as:

$$\mathrm{Di} = \sum_{k=1}^{y} \mathbf{Pi}, k \ln(\mathbf{Pi}, k)$$

where y is the number of subdivisions or bins in the cell scaling (= 50) if the cell c_i contains a continuous variable, and Pi is the abundance vector on any map at cell c_i such that,

$$\mathbf{Pi} = \{Pi, 1, Pi, 2 \ldots Pi, y\}, \mathbf{Pi} \in [0, 1].$$

The fractal dimension was calculated as:

$$\mathrm{D_{frac}} = \begin{cases} \text{if } \frac{\mathrm{S_{peri}}}{u} > 4 : \frac{\mathrm{S_{size}}}{u^2} \log\left(\frac{\mathrm{S_{peri}}/u}{4}\right), \\ \text{if } \frac{\mathrm{S_{peri}}}{u} = 4 : \qquad 2 \end{cases}$$

where s_{peri} and s_{size} are the perimeter length and patch size (area) of identified groups of contiguous cells (including diagonal cells) and 'holes' in patches. For this raster mapping, the cells (c_i) are unit-spaced and therefore $u = 1$. The indices are computed for all cells in a radius neighborhood of 12 cells from the cell of interest in a sliding boxcar across the map and a weighted mean is computed for each cell and for the map in total (see details in Hagen-Zanker 2006, and discussion in Rose *et al.* 2008 for oceanographic applications).

Map similarity comparisons were based on the Numerical Fuzzy Kappa (NFK) measure (Hagen 2003; Hagen-Zanker 2006), which produces a statistic that represents the difference in average similarity between maps. All computations are contingent on the reasonable *a priori* assumption that the map data are spatially autocorrelated (Legendre & Fortin 1989; Fernandez *et al.* 2009). NFK is an extension of the original Kappa algorithm based on a misclassification matrix between map cells (*i.e.* Monseurd & Leemans 1992) but uses the weighted inputs of neighboring cells to compute the Kappa statistic based on fuzzy set theory. In this manner, the measure of cell similarity is continuous across the map based on the value and distance of neighboring cells (in this case with a Gaussian weighting, and with a 12-cell neighborhood). The final NFK statistic quantifies levels of map difference and models a human measurement of map similarity more closely than the original Kappa (Pontius 2000; Hagen-Zanker *et al.* 2005; Rose *et al.* 2009; Fernandez *et al.* 2009). The

NFK statistic varies between 0 and 1, with greater values indicating a higher degree of similarity (1 being identical).

Results

As shown in Fig. 3A, the benthic water temperature on Conch Reef varies with season and depth. The yearly mean and standard deviation of the temperature at 10, 20 and 30 m depth is 26.60 ± 2.43, 26.49 ± 2.38 and 26.22 ± 2.35 °C, respectively. The yearly minimum and maximum temperatures, like the mean temperatures, are similar across the 10, 20 and 30 m depths; however, the summary data averaged from a single point in space do not adequately describe the spatial and temporal heterogeneity in the temperature field along the reef. The minimum and maximum temperature was 21.60 and 30.81 °C at 10 m depth, 22.04 and 30.72 °C at 20 m depth, and 21.67 and 30.54 °C at 30 m depth. In the summer months the water column at Conch reef is strongly stratified with respect to temperature and density. Superimposed on the general warming of the surface layers is high frequency variability associated with incursions of cold, deep water up the reef slope (Fig. 3A,B), often in the form of distinct fronts. These temperature fluctuations can be as great as 6–8 °C and can occur on a time scale of just a few minutes. Temperature variability is greatest at the base of the reef slope (Fig. 3C) and the deeper depths are associated with the lowest mean temperatures because not all coldwater fronts advect all the way up the reef slope. The coldest minimum temperatures are also found at the deepest depths; however, it should be noted that there are still periods when the entire water column, from the 30 m isobath to the surface, is isothermal (particularly mid-October through February) and may exceed 30 °C (*i.e.* during August and September).

There are variations in reef benthic temperature that are independent of depth. As shown in Fig. 4, non-zero values of the horizontal mean temperature anomaly, mapped onto the reef bathymetry, imply site-specific deviations from the mean profile of temperature at a given depth. The anomalous temperatures along the 18–20 m isobath are associated with variations in temperature in and around the 2–3 m depression in the reef (in the approximate center of the BOA array). During this sampling interval, quadrant B (noted in Fig. 2) was, on average, approximately 1 °C warmer than areas of similar depth (*i.e.* quadrant A). Reef locations nearer the base of the reef slope, deeper than about 22 m, show little horizontal variation in temperature.

As shown in Fig. 5, the distribution of benthic organisms is highly patchy. On Conch reef, the spatially dominant epilithic organisms are a suite of turf and macro 'fleshy' algae (including the sampled *Dictyota menstrualis* and *Halimeda tuna*,). In a few locations, macroalgal coverage exceeded 40%. At this reef site on the sand plain deeper than about 30 m, the bottom is colonized by many large individual seaweeds, including *Codium* sp., *Caulerpa* sp., *Halymenia* sp. and *Kallymenia* sp. (see also Leichter *et al.* 2008). Living hermatypic coral coverage (primarily *Montastrea* spp., *Agaricia* spp. and *Porities* spp.) varied between 0 and about 25% depending on the location, as did the coverage of large epilithic sponges (primarily *Xestospongia muta, Spheciospongia vesparium*, and *Scopalina reutzleri*). It is worth noting that although algae, coral and sponges do colonize suitable substrate together, the highest percent coverage areas tend to be in non-overlapping patches.

The patterns of algal isotopic composition are complex (Fig. 6). The inorganic $\delta^{13}C$, $\delta^{15}N$ signatures for both *H. tuna* and *D. menstrualis* vary both within and across depth gradients on spatial scales of 10–20 m. There is some indication of a depth dependence in *D. menstrualis* $\delta^{15}N$, which shows more negative signatures in water deeper than about 20 m. The $\delta^{15}N$ signature appears less depth-dependent, and values are slightly enriched along the topographic high in quadrants D and A. The inorganic oxygen isotopic signature $\delta^{18}O$, from *H. tuna* calcium carbonate sampling (Fig. 7), indicates higher values along the fore reef slope into deeper water (in areas of greater benthic water temperature variability) and lowest (quadrant B) in the shallower sampling regions. The spatial patterns of the C:N ratio in *H. tuna* and *D. menstrualis* are equally complex. Both show higher ratios in quadrants C and B and in deeper water; however, there is variability along isobaths, and the C:N ratio is lower for *H. tuna* (7–20) than for *D. menstrualis* (10–30) even from collocated samples.

The descriptive metrics of map structure – the fractal dimension (D_{frac}) and the Shannon entropy index (D_i) – are summarized in Table 1. In each case, both metrics seem to reasonably mirror the properties that can be noted subjectively by a visual map comparison. The relatively complex and patchy distribution of sponge percent area coverage (Fig. 5) is reflected in the high value of $D_{frac} = 1.81$, whereas the relatively less patchy and convoluted mapping of *H. tuna* $\delta^{18}O$ (Fig. 7) has a slightly lower $D_{frac} = 1.59$. Similarly, the measure of compositional complexity, D_i, is greatest for those maps showing a great range and diversity in map cell parameter values, such as algae percent coverage (Fig. 5, $D_i = 3.53$) *versus* percent coral coverage ($D_i = 3.01$), which was dominated in the surveyed area by a just a few patches of coral growth. It should be noted that not all the measured environmental parameters (*i.e.* temperature means) are

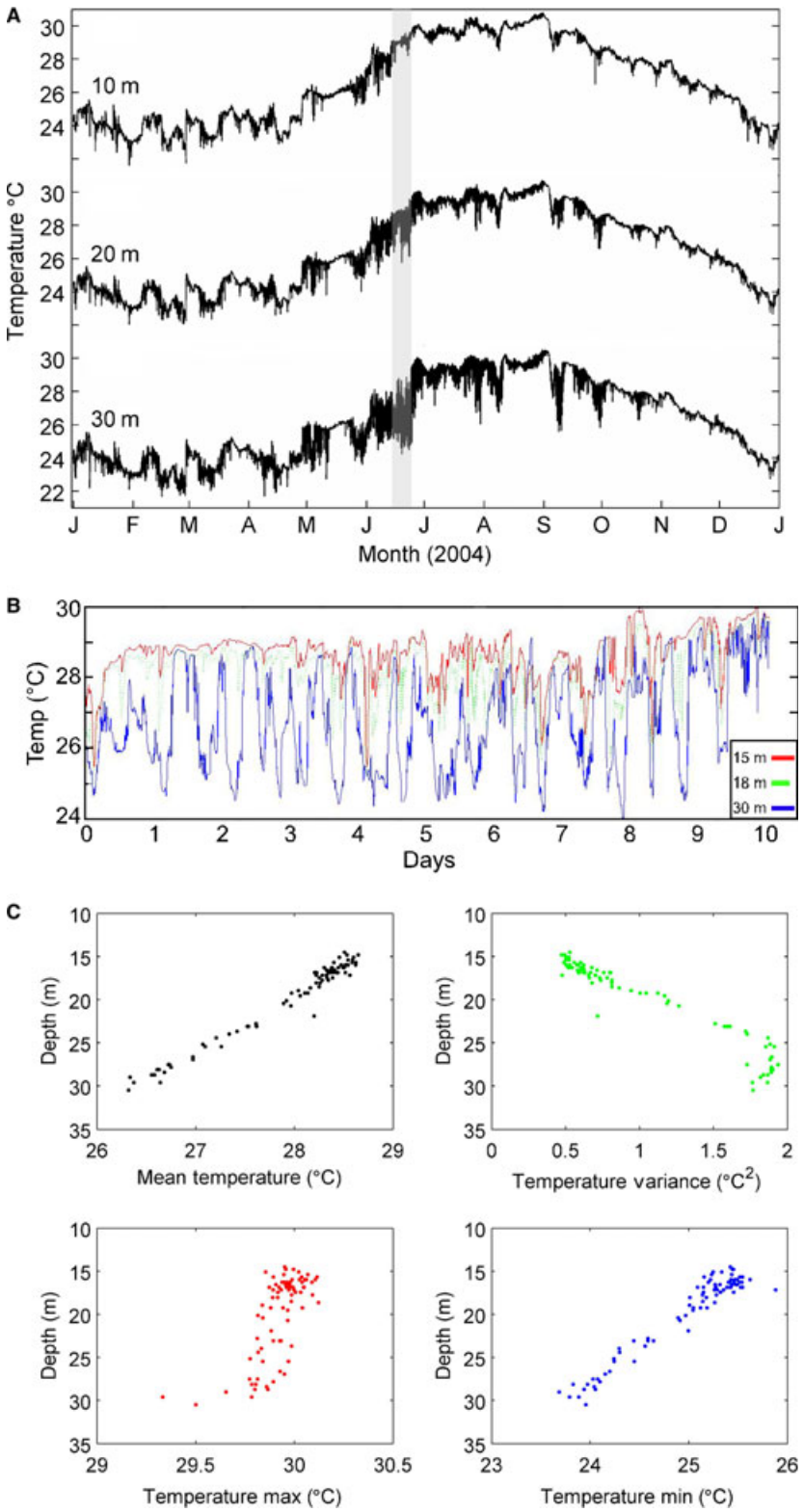

Fig. 3. (A) One-year segment of benthic water temperature from 10, 20 and 30 m depth on Conch Reef during 2004. Data were sampled at 2-min intervals and averaged in 10-min bins to plot the complete dataset. The shaded time period in June corresponds to the BOA node temperature data subset plotted in (B). (B) 10-day segment of benthic water temperature from three selected nodes commencing 12:00 h on 10 June 2004. The upper red line was sampled at approximately 15 m depth (point B in Fig. 2), green dotted line at 18 m depth (near upper edge of fore reef slope, point E in Fig. 2) and the blue line at 30 m depth (point C in Fig. 2). Node temperature sensors are sampled at 5-s intervals. (C) Mean, maximum, minimum and variance in benthic water temperature *versus* depth across the entire BOA array (June 2004). Node temperatures were sampled at 5-s intervals.

included here as separate spatial figure maps; however, the descriptive statistics from the spatial analysis are listed in Table 1 and summarized in Fig. 3C. Detailed spatial maps of temperature parameters on Conch Reef and their variation through time, can be found in (Leichter *et al.* 2005).

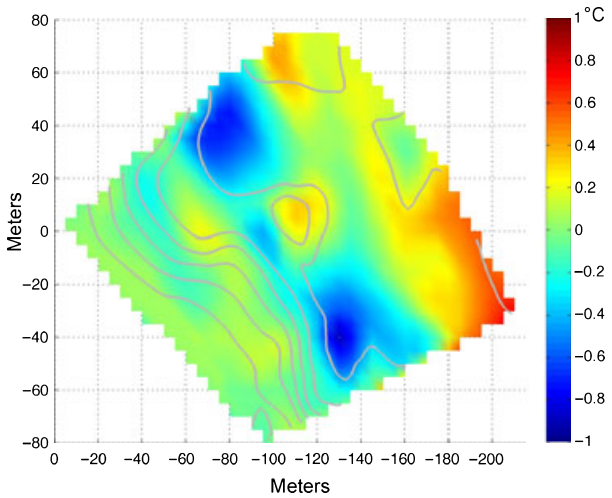

Fig. 4. Mean horizontal temperature anomaly June–September 2004, interpolated onto the reef bathymetry. Gray lines indicate bathymetric contours as in Fig. 2.

The results of the NFK similarity comparisons between spatial maps are summarized in Table 1. The NFK indices reflect the overall 'similarity' of different maps to each other, much like subjective visual comparison. It must be remembered that in calculating the NFK, the parameter data are normalized and that the color scales in Figs 2–7 are not, and are instead optimized for individual datasets. Although most of the map pairs show a degree of similarity, some NFK trends are notable. Spatial maps of algae, coral and sponge coverage are not very similar to each other, nor are they very similar to spatial maps of bathymetry or temperature parameters. Some spatial comparisons between *D. menstrualis* and *H. tuna* isotopic variability with depth and temperature show higher similarity. For example, *H. tuna* δ^{13}C shows higher NFK indices with depth and temperature maxima (0.57 and 0.66, respectively). Some of these similarities are indicated in bold type in Table 1 and are reflected in the DISTLM model in Table 2.

Results of the DISTLM model of community composition based on a Bray–Curtis resemblance matrix using percent coral, algae and sponges revealed very low explanatory value for the metrics used (depth, temperature minimum, maximum, mean and variance; $r^2 < 0.08$). In this model set, depth had the greatest explanatory value. Models of environmental correlates to isotopic variability yielded more statistical explanatory power. Here the temperature minimum was in the top model sets as a statistical predictor of variability in δ^{15}N for both *H. tuna* and *D. menstrualis*, although again, r^2 values were generally low for these models. Variability in δ^{13}C for *H. tuna* and *D. menstrualis* showed slightly stronger statistical relationships with environmental variables with depth and

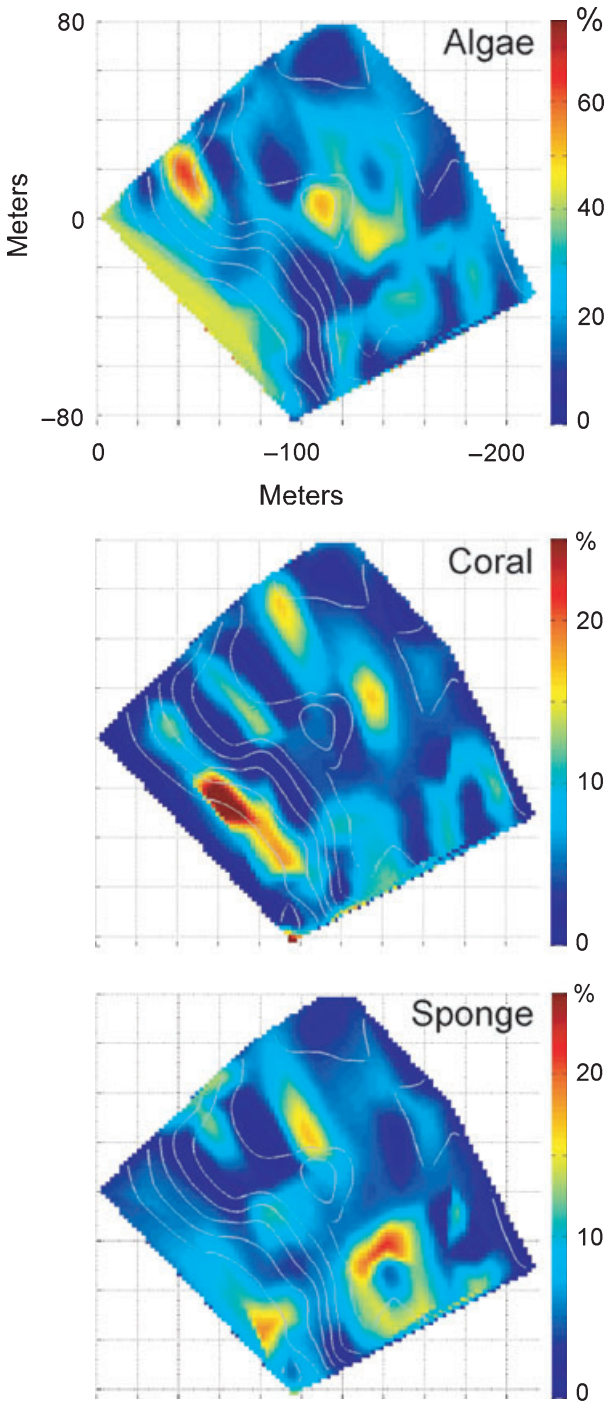

Fig. 5. Percent benthic coverage of macro and turf algae (top), hermatypic corals (middle) and epilithic sponges (bottom). Note change in percent scale for each group.

temperature minima included in the top model sets. Variability in δ^{18}O of calcium carbonate in *H. tuna* was best explained statistically by variability in temperature and in the temperature maxima. Results of the best two solutions

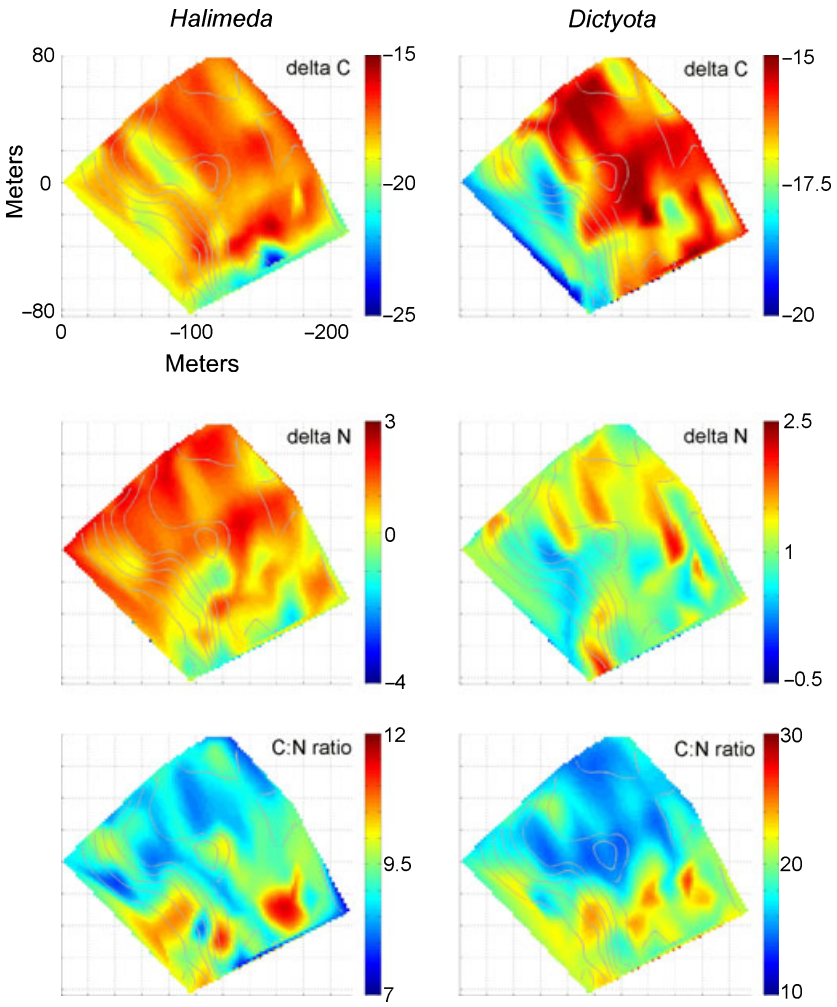

Fig. 6. Algal tissue isotope signatures, $\delta^{13}C$ (top), $\delta^{15}N$ (middle), and the C:N ratio (bottom) across the study site for *Halimeda* sp. (left) and *Dictyota* sp. (right). Color scale indicates standard delta notation. Gray lines indicate bathymetric contours as in Fig. 2.

evaluated by AICc for each biological factor and the environmental variables included in the model are shown in Table 2.

Discussion

The ability to measure the physical environment at a scale of tens of meters over a 12,000-m^2 grid and concomitantly to sample community and primary producer isotopic composition at the same spatial resolution provides a unique view of the physical and biological heterogeneity of a coral reef under ambient physical forcing. Spatial mapping of temperature metrics onto the reef topography and calculation of within-depth thermal anomalies reveal persistent areas of relative cooling and warming. Spatial mapping of the node-specific biological sampling also reveals domain-scale heterogeneity in community and isotopic metrics. Two environmental factors, depth and mean temperature, explain a significant portion of the variance in *Dictyota* $\delta^{13}C$, while the two factors mean temperature and variance in temperature explain a significant portion of the variance in *Halimeda* $\delta^{13}C$. The other measured biological factors are highly variable across the reef surface but not well explained by the variation in depth or temperature metrics. The high degree of environmental and biological heterogeneity within depths is an intriguing observation and may raise important caveats to simple interpretations of apparent depth effects in cases where this level of extensive sampling within depths may be absent due to sampling or experimental design limitations.

Estimates of the flux of inorganic nutrients across the reef slope suggest increases of more than an order of magnitude may occur during summer upwelling events relative to other periods (Leichter *et al.* 2003), and high frequency upwelling appears to be a significant overall nutrient source for the outer reef slopes (Boyer & Jones 2002; Kruczynski & McManus 2002; Leichter *et al.* 2003).

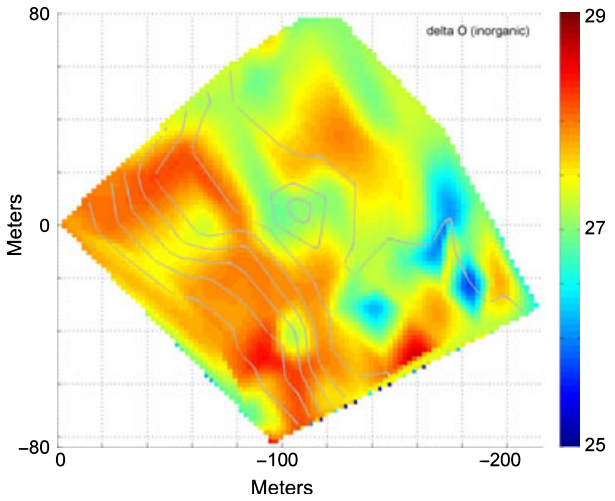

Fig. 7. Oxygen isotopic signature, $\delta^{18}O$, across the study site, from the calcium carbonate component of the *Halimeda* sp. samples (see text). Scale indicates standard delta notation. Gray lines indicate bathymetric contours as in Fig. 2.

Figure 3 illustrates the variability associated with frequent incursions of cool, subthermocline water onto the reef slopes particularly in summer. Sampling of the water column seaward of the FLKRT indicate that offshore water that is approximately 25–26 °C and cooler showed a nearly linear increase in total inorganic nitrogen with decreasing temperature. Leichter *et al.* (2003, 2008) used calculations of total degree cooling hours below 26 °C as an index of net nutrient exposure for benthic macroalgae. The thermocline seaward of the FLKRT is often relatively shallow (*e.g.* 50 m depth), especially in summer, and upward incursions of cool (22–26 °C) water onto reef slopes occur frequently. These are readily apparent in the temperature records illustrated in Fig. 3. The relatively high concentrations of subsurface nitrate (5–20 μM) and soluble reactive phosphate (0.1–2.0 μM) below the thermocline (Lee *et al.* 1985; Leichter *et al.* 2003) clearly points to the potential for the offshore subsurface nutrient pool to be an important source of nutrients reaching the reef slope, especially at depths of >10 m as incoming internal waves mix subthermocline water with warmer surface waters.

Incidental internal waves interact with reef topography, producing significant heterogeneity in cool water exposure and residence times within, as well as across, depths (Leichter *et al.* 2005). The horizontal temperature anomaly is strongly associated with ridges and depressions that restrict the movement of cooler, denser and nutrient-rich waters (*i.e.* Fig. 4). Reef topography first interacts with the advecting, incoming wave fronts and then guides gravity-driven density flows after the fronts have passed. A growing body of evidence supports the general

Table 1. Comparison of spatial maps (Figs 4–7) based on the Numerical Fuzzy Kappa (NFK) statistic. Larger values indicate a greater degree of map similarity. The fractal dimension (a measure of patch complexity) and the Shannon entropy index (a measure of map compositional diversity) for each map are indicated for each spatial mapping. NFK indices in bold correspond to factors selected by DISTLM as the best explanatory variables, as shown in Table 2.

			Numerical Fuzzy Kappa similarity index															
Spatial mapping	Fractal dimension	Diversity index	Depth	Algae cover	Coral cover	Sponge cover	*Dictyota* C:N ratio	*Dictyota* $\delta^{13}C$	*Dictyota* $\delta^{15}N$	*Halimeda* C:N ratio	*Halimeda* $\delta^{13}C$	*Halimeda* $\delta^{15}N$	*Halimeda* $\delta^{18}O$	Temp max	Temp mean	Temp min	Temp var
Depth	1.68	3.50	1.00														
Algae cover	1.76	3.53	0.55	1.00													
Coral cover	1.72	3.01	0.49	0.44	1.00												
Sponge cover	1.82	3.51	0.53	0.57	0.48	1.00											
Dictyota C:N ratio	1.63	3.59	0.54	0.58	0.40	0.56	1.00										
Dictyota $\delta^{13}C$	1.77	3.15	**0.55**	0.52	0.51	0.51	0.53	1.00									
Dictyota $\delta^{15}N$	1.60	3.40	0.47	0.57	0.31	0.54	0.55	0.41	1.00								
Halimeda C:N ratio	1.81	3.45	0.55	0.64	0.35	0.56	0.60	0.44	0.67	1.00							
Halimeda $\delta^{13}C$	1.65	3.54	**0.57**	0.61	0.37	0.55	0.58	0.44	0.65	0.70	1.00						
Halimeda $\delta^{15}N$	1.77	3.71	0.45	0.56	0.29	0.46	0.46	0.37	0.68	0.59	0.60	1.00					
Halimeda $\delta^{18}O$	1.59	3.41	0.52	0.56	0.21	0.40	0.52	0.31	0.67	0.61	0.60	0.68	1.00				
Temp max	1.77	2.85	0.48	0.63	0.38	0.59	0.56	0.47	0.72	0.69	**0.66**	0.59	**0.51**	1.00			
Temp mean	1.46	3.07	0.36	0.49	0.31	0.47	0.45	**0.32**	0.70	0.60	0.56	**0.62**	0.61	0.65	1.00		
Temp min	1.44	3.17	0.37	0.50	0.32	0.49	0.46	0.33	0.70	0.62	**0.56**	**0.60**	0.59	0.69	0.89	1.00	
Temp var	1.47	3.22	0.80	0.59	0.44	0.58	0.55	0.50	0.51	0.61	0.63	**0.49**	**0.52**	0.52	0.39	0.40	1.00

Table 2. DISTLM best solutions for linear model sets relating biological factors (column 1) to a set of predictor environmental variables from the bathymetry and temperature sensor node data. Environmental variables are coded as (1) depth, (2) temperature maximum, (3) temperature mean, (4) temperature minimum and (5) temperature variance. Akaike's information criteria (AIC) corrected for multiple predictor variables are shown as AICc values, along with r^2 and residual sum of squares. For each factor, the top overall models are shown.

Factor	AICc	r^2	RSS	Model Selection
Community composition	542.54	0.06	65171	1,5
	543.46	0.02	67735	1
Halimeda tuna δ^{15}N	−26.18	0.13	51.8	3,4,5
	−25.92	0.10	53.5	3,4
Halimeda tuna δ^{13}C	37.06	0.13	117.5	1,4
	38.85	0.14	116.8	1,2,4
Halimeda tuna δ^{18}O	−114.4	0.28	18.2	5
	−113.5	0.29	17.9	2,5
Dictyota menstrualis δ^{15}N	−156.9	0.02	10.7	4
	−156.8	0.02	10.7	2
Dictyota menstrualis δ^{13}C	−42.9	0.47	44.5	3
	−42.6	0.46	44.6	1

hypothesis that exposure to the offshore nutrient pools has important consequences for benthic primary producers in this system. Both Vroom *et al.* (2003) and Smith *et al.* (2004) found increased growth rates of the green alga *Halimeda tuna* with increasing depth on the slope of Conch Reef. Smith *et al.* (2004) also found that *H. tuna* at 7 m depth showed a significant response in nutrient addition experiments, whereas individuals at 21 m depth showed no response, suggesting that these deeper individuals existed in nutrient-replete conditions. Isotopic evidence also suggests utilization of the pulses of subthermocline nitrate by a common benthic macroalga, *Codium isthmocladum*. Leichter *et al.* (2003) found that δ^{15}N values of *C. isthmocladum* increased from approximately +2.0% at 9 m depth to +5.0% at 35 m, corresponding to increasing exposure to pulses of subthermocline water and thus a gradient in availability of offshore nitrate with depth.

However, simple trends with depth are not apparent in the spatial mapping of δ^{15}N of *H. tuna* or *Dictyota menstrualis* shown here. Instead, δ^{15}N varied as much along isobaths as across the depth range sampled (approximately 13–30 m). One reason for the lack of apparent relationship between δ^{15}N and depth or temperature metrics may be the algal physiological state with respect to nitrogen needs during growth. Considering the C:N ratios as a partial indicator of nitrogen status, we see that C:N is consistently low across the reef for *H. tuna* and quite variable for *D. menstrualis*. Low and highly variable C:N may suggest the algae were not strongly nitrogen-limited, and instead may have experienced relatively nutrient-replete conditions under which we would not expect a tight coupling between location and δ^{15}N. The spatial distribution of the taxa sampled here and the variability in isotopic composition does not show a simple relationship with depth or with the variation in benthic temperature field. Again, we see that when sampling at fine spatial scales there is extensive variance which is not visible in courser sampling that only encompasses the main physical gradient, depth.

Although the possibility of nutrient transport via submarine groundwater movement through the Florida Keys carbonate platform has been investigated, tracer experiments (Corbett *et al.* 2000; Dillon *et al.* 2003), near bottom salinity and temperature data (Leichter *et al.* 1996, 2003), or radium isotopic measurements have not shown evidence of groundwater delivery to the reef tract (Paytan *et al.* 2006). Attempts to infer nutrient pollution sources from δ^{15}N measurements in tissues of gorgonians have also been made on reefs both nearshore and several kilometers from shore in the Florida Keys (Lapointe *et al.* 2004; Ward-Paige *et al.* 2005). These studies did not include determination of δ^{15}N values for the purported nutrient sources, relying instead on the hypothesis that tissue δ^{15}N values of 3–4‰ indicate land-based nutrient pollution (Lapointe *et al.* 2004). In the same region, however, Swart *et al.* (2005) found no clear signals in coral δ^{15}N from offshore to nearshore reefs, but did find significant temporal variation, suggesting seasonal changes in the relative importance of coral autotrophy and heterotrophy. Our findings of high spatial variation in macroalgal δ^{15}N sampled at small scales and lack of clear relationships to depth or temperature metrics reinforce the findings of Swart *et al.* (2005) as well as Lamb & Swart (2008) who found no clear patterns in δ^{15}N for corals or particulate organic material across the FLKRT and conclude that δ^{15}N data in this system do not indicate clear spatial gradients in anthropogenic nutrient loading.

Analysis of δ^{18}O from calcifying algae, particularly from *Halimeda* sp. sediment fragments, has been used to find evidence of water temperature fluctuations and cool water periods during the Holocene (Holmes 1982). In fact, Holmes (1982) found evidence of an approximately 4 °C cooler period centered roughly 4,000 years before the present in the Northeast Caribbean. Essentially, as we

cannot measure prior temperatures directly, the paleo $\delta^{18}O$ record from carbonates preserved in sediments can be used to infer prior temperatures. In our study, by contrast, we have directly measured the spatial variation in both the temperature field and the $\delta^{18}O$ composition of recently deposited calcium carbonate in living *H. tuna*. A variety of empirical formulations (*e.g.* Grossman & Ku 1981, 1986) have been developed to model temperature from knowledge of $\delta^{18}O$ in organismal aragonite or calcite pools and assumptions about salinity and seawater $\delta^{18}O$. We can use our data to compare measured temperatures with the temperature we would predict across the reef surface based on *H. tuna* $\delta^{18}O$ and estimates of $\delta^{18}O$ for the offshore waters of the Florida Keys (Schmidt *et al.* 1999).

Holmes (1983), following Grossman & Ku (1981), modeled temperature, T, at the time of *Halimeda* carbonate formation as:

$$T = 19 - 3.52(\delta - A) + 0.03(\delta - A)^2$$

where δ is the $\delta^{18}O$ value of the carbonate (relative to PDB) and A is the $\delta^{18}O$ value of the seawater (SMOW). In Holmes (1983), $\delta^{18}O$ for modern *Halimeda* from the Virgin Islands ranged from −2.5 to −2.0 ‰ (mean −2.15‰), yielding predicted temperatures ranging from 26.7 to 28.9 °C which were close to measured values for the area, assuming the seawater $\delta^{18}O$ to be close to 0 ‰. Holmes (1983) also reported *Halimeda* $\delta^{18}O$ values of −3.3 to −3.0 ‰ for Marquesas Keys (Florida) corresponding to predicted temperatures of 29.8–31.0 °C, also considered within the range of actual temperatures at their sites.

In our study at Conch Reef, we found *H. tuna* $\delta^{18}O$ ranging from −5.06 to −2.07 with mean −3.36‰. Using the equation of Grossman & Ku (1981) and a seawater $\delta^{18}O$ of +1.0 estimated from Schmidt *et al.* (1999) yields predicted temperatures ranging from 30.0 to 41.4 °C with mean of 34.9 °C. These temperatures are significantly in excess of measured temperatures at the site. Another way to interpret these data is that the measured $\delta^{18}O$ values in the *H. tuna* aragonite were lower (less enriched in ^{18}O) than would be expected based on estimates of the average seawater $\delta^{18}O$ for the Florida Straits and known temperatures at the site. If, instead, we assume a lower value of seawater $\delta^{18}O$, −1.5‰, we attain a more reasonable range of predicted temperatures, 22.8–33.8 °C with mean of 27.5 °C. Figure 8 shows the predicted temperature at each sampling node under this scenario plotted against the measured node mean temperature. Under the modeling assumptions, the relatively low (less enriched) $\delta^{18}O$ values we find for *H. tuna* carbonate material therefore imply that seawater $\delta^{18}O$ is approximately 2.5‰ lower than

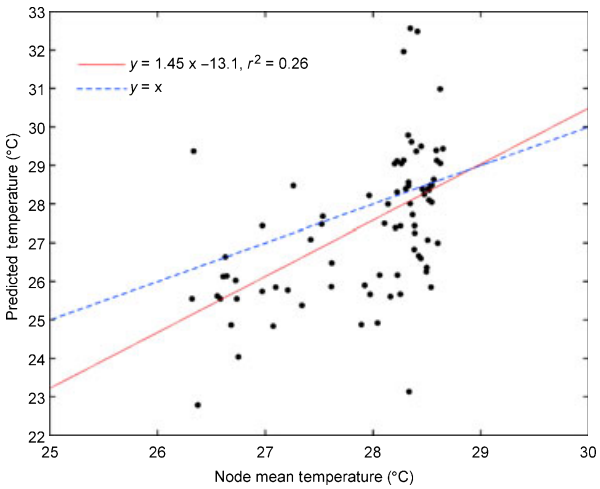

Fig. 8. Comparison of predicted temperature from *Halimeda tuna* $\delta^{18}O$ signature following Holmes (1982) and Grossman & Ku (1981) *versus* the mean node temperature measured by the BOA. Temperature here is modeled using a value of −1.0‰ for seawater $\delta^{18}O$. Upper dotted line indicates 1:1 ratio between predicted and measured temperatures; solid line is the least-mean-squares linear fit T_{pred} = 1.45-T_{obs}–13.122, r^2 = 0.26.

expected based on observed values for the offshore waters of the Florida Keys. Fresh water input is a possible source for low seawater $\delta^{18}O$ values (Ren *et al.* 2002). Thus, the relatively light $\delta^{18}O$ signatures for *H. tuna* carbonate (which can also be seen in Fig. 7) may be indicative of freshwater input into this system, perhaps via frequent heavy rainfall and potentially from inshore or underground sources with depleted levels of ^{18}O, such as the Florida aquifer (Lloyd 1964; Swart *et al.* 1996, although groundwater input had not been identified in prior nutrient flux studies).

More important, our data reveal large spatial variation in contemporary carbonate $\delta^{18}O$ values within a relatively small spatial area. In fact, as shown in Fig. 8, a linear fit between predicted and observed temperatures only explains approximately 25% of the variance. This suggests that the modeling approach used to estimate temperatures from carbonate $\delta^{18}O$ may not adequately represent the calcification dynamics under a fluctuating thermal environment. If, for example, *H. tuna* calcification rate varies in some non-linear manner with rapid changes in temperature (and nutrients), then predicted temperatures based on a mean $\delta^{18}O$ from a homogenized sample may not reflect the time-varying environmental signal. Greater understanding of the potential sources of heterogeneity in contemporary carbonate biogeochemistry may improve our understanding of the importance of integrating variation and spatial heterogeneity into analysis of paleo carbonates and modeled paleo climate indicators. This study

clearly points to the potential for large variation in carbonate $\delta^{18}O$ values within a small spatial scale on a contemporary coral reef. For areas with highly dynamic thermal environments and exposure to variation associated with internal waves in the past, we might expect similar large spatial (and temporal) variation in $\delta^{18}O$ recorded in preserved carbonates.

Conclusions

The interaction of oceanographic forcing and heterogeneous topography at Conch Reef results in highly variable physical and ecological patterns at small scales in this coral reef ecosystem. Benthic temperatures show high-frequency fluctuations associated with the advection of internal waves that transport cold, nutrient rich water across the reef slope. The nutrient field available to reef organisms is dynamically modified by the FLKRT hydrography and local topography. The patchy distribution of key benthic species must be considered in terms of topography, complex ecological interactions and variations in the physical environment. The spatial distribution of sponges, hermatypic corals and macroalgae over a length scale of approximately 100 m and the sampled macroalgal stable isotopes, C, N, O are all highly variable and not necessarily determined by depth along the reef slope – nor are they strongly correlated with water temperature variability or the distribution of different taxa as indicated by only weak explanatory power in DISTLM models of community composition and in an independent analysis of spatial similarity based on the map comparisons using the NFK. The divergence in measured and the predicted temperatures from the $\delta^{18}O$ carbonate signature, as well as the relatively light $\delta^{18}O$ signatures may indicate freshwater input at the Conch Reef site. Additionally, this divergence, even among closely located samples, indicates the requirement to sample this spatial heterogeneity in contemporary as well as paleontological studies.

Acknowledgements

We thank the following people for supporting this research: S. Miller and personnel at the National Undersea Research Center in Key Largo, Florida, as well as divers A. Coyac, C. Zilberger, S. Curless, G. Deane, M. Murray and boat captains M. Birns and K. Boykin. J. Uyloan and C. Humphries assisted in the fabrication and calibration of the BOA array. L. Jack assisted with statistical analyses. Funding for the field research was provided by NSF (OCE 0239449, 0220400) and NOAA UNCW/NURC.

References

Altabet M.A. (2001) Nitrogen isotopic evidence for micronutrient control of fraction NO_3 utilization in the equatorial Pacific. *Limnology and Oceanography*, **46**, 368–380.

Altabet M.A. (2005) Isotopic tracers of the marine nitrogen cycle. In: Volkman J. (Ed.), *Marine Organic Matter: Chemical and Biological Markers, Vol 2, The Handbook of Environmental Chemistry*. Elsevier, Amsterdam: 251–293.

Anderson M., Gorley R., Clarke K. (2008) *PERMANOVA+ for PRIMER: Guide to Software and Statistical Methods*. University of Auckland, Auckland, New Zealand: 214 pp.

Atkinson M.J., Bilger R.W. (1992) Effects of water velocity on phosphate uptake in coral reef-flat communities. *Limnology and Oceanography*, **37**, 273–279.

Boyer J.N., Jones R.D. (2002) A view from the bridge: external and internal forces affecting the ambient water quality of the Florida Keys Marine Sanctuary. In: Porter J.W., Porter K.G. (Eds), *The Everglades, Florida Bay, and Coral Reefs of the Florida Keys. An Ecosystem Sourcebook*. CRC Press, Boca Raton: 609–628.

Brown B.E. (1997) Coral bleaching: causes and consequences. *Coral Reefs*, **16**, S129–S138.

Burnham K., Anderson D. (2002) *Model Selection and Multimodel Inference: A Practical Information-Theoretic Approach*, 2nd edn. Springer-Verlag, New York.

Cole M.L., Kroeger K.D., McClelland J.W., Valiela I. (2005) Macrophytes as indicators of land-derived wastewater: application of delta N-15 method in aquatic systems. *Water Resource Research*, **41**, 1–9.

Corbett D.R., Dillon K., Burnett W., Chanton J. (2000) Estimating the groundwater contribution into Florida Bay *via* natural tracers ^{222}Rn and CH_4. *Limnology and Oceanography*, **45**, 1546–1552.

Cornelisen C., Wing S., Clark M., Bowman M., Frew R., Hurd C. (2007) Patterns of macroalgal stable carbon and nitrogen isotope signatures: interaction between physical gradients and nutrient source pools. *Limnology and Oceanography*, **52**, 820–832.

Davis K., Leichter J., Hench J., Monismith S. (2008) Effects of western boundary current dynamics on the internal wave field of the Southwest Florida shelf. *Journal of Geophysical Research*, **113**, C09010.

Dayton P.K. (1985) Ecology of kelp communities. *Annual Review of Ecology and Systematics*, **16**, 215–245.

Deane G., Stokes M.D. (2002) A robust single-cable sensor array for oceanographic use. *IEEE Journal of Oceanic Engineering*, **27**, 760–767.

D'Elia C.F., Wiebe W.J. (1990) Biogeochemical nutrient cycles in coral-reef ecosystems. In: Dubinsky Z. (Ed.), *Ecosystems of the World, Vol 25: Coral Reefs*. Elsevier, Amsterdam: 49–74.

Dillon K., Burnett W., Guebuem K., Chanton J., Corbett D.R., Elliott K., Kump L. (2003) Groundwater flow and phosphate

dynamics surrounding a high discharge wastewater disposal well in the Florida Keys. *Journal of Hydrology*, **284**, 193–210.

Fernandez M., Blum S., Reichle S., Guo Q., Holzman B., Hamilton H. (2009) Locality uncertainty and the differential performance of four common niche-based modelling techniques. *Biodiversity Informatics*, **6**, 36–52.

Fourqurean J.W., Moore T.O., Fry B., Hollibaugh J.T. (1997) Spatial and temporal variation in C:N:P ratios, delta N-15 and delta C-13 of eelgrass *Zostera marina* as indicators of ecosystem processes, Tomales Bay, California, USA. *Marine Ecology Progress Series*, **157**, 147–157.

Grossman E.L., Ku T.L. (1981) Aragonite-water isotopic paleotemperature scale base on benthic foraminifera, *Hoeglundia elegans*. *Abstract: Geological Society of America*, **13**, 464.

Grossman E.L., Ku T.L. (1986) Oxygen and carbon fractionation in biogenic aragonite. *Chemical Geology*, **59**, 59–74.

Hagen A. (2003) Fuzzy set approach to assessing similarity of categorical maps. *International Journal of Geographical Information Science*, **17**, 235–249.

Hagen-Zanker A. (2006) Map comparison methods that simultaneously address overlap and structure. *Journal of Geographical Systems*, **8**, 165–185.

Hagen-Zanker A., Straatman B., Uljee I. (2005) Further developments of a fuzzy set map comparison approach. *International Journal of Geographical Information Science*, **19**, 769–785.

Hansson S., Hobbie J.E., Elmgren R., Larsson U., Fry B., Johansson S. (1997) The stable isotope ratio as a marker of food-web interactions and fish migration. *Ecology*, **78**, 2249–2257.

Hepburn C.D., Pritchard D.W., Cornwall C.E., McLeod R.J., Beardall J.B., Raven J.A., Hurd C.L. (2011) Diversity of carbon use strategies in macroalgal communities: implications for a high CO_2 ocean. *Global Change Biology*, **7**, 2488–2497.

Holmes C.W. (1983) $\delta^{18}O$ variations in the *Halimeda* of Virgin Island sands: evidence of cool water in the northeast Caribbean, Late Holocene. *Journal of Sedimentary Petrology*, **53**, 429–438.

Knowlton N., Jackson J.B. (2001) The ecology of coral reefs. In: Bertness M.D., Gaines S.D., Hay M.E. (Eds), *Marine Community Ecology*. Sinauer Associates, Inc., Sunderland, MA: 385–422.

Kruczynski W.L., McManus F. (2002) Water quality concerns in the Florida Keys: sources effects, and solutions. In: Porter J.W., Porter K.G. (Eds), *The Everglades, Florida Bay, and Coral Reefs of the Florida Keys. An Ecosystem Sourcebook*. CRC Press, Boca Raton: 827–881.

Kübler J., Raven J. (1994) Consequences of light limitation for carbon acquisition in three rhodophytes. *Marine Ecology Progress Series*, **110**, 203–209.

Lamb K., Swart P.E. (2008) The carbon and nitrogen isotopic values of particulate organic material from the Florida Keys: a temporal and spatial study. *Coral Reefs*, **27**, 351–362.

Lapointe B.E., Matzie W.R., Barile P.J. (2004) Anthropogenic nutrient enrichment of seagrass and coral reef communities in the Lower Florida Keys: discrimination of local *versus* regional nitrogen sources. *Journal of Experimental Marine Biology and Ecology*, **308**, 23–58.

Lee T.N., Mayer D.A. (1977) Low-frequency current variability and spin-off eddies along shelf off Southeast Florida. *Journal of Marine Research*, **35**, 193–220.

Lee T.N., Schott F.A., Zantopp R. (1985) Florida current – low-frequency variability as observed with moored current meters during April 1982 to June 1983. *Science*, **227**, 298–302.

Legendre P., Fortin M.-J. (1989) Spatial pattern and ecological analysis. *Vegetation*, **80**, 107–138.

Leichter J.J., Wing S.R., Miller S.L., Denny M.W. (1996) Pulsed delivery of subthermocline water to Conch Reef (Florida Keys) by internal tidal bores. *Limnology and Oceanography*, **41**, 1490–1501.

Leichter J.J., Shellenberger G., Genovese S.J., Wing S.R. (1998) Breaking internal waves on a Florida (USA) coral reef: a plankton pump at work? *Marine Ecology Progress Series*, **166**, 83–97.

Leichter J.J., Stewart H.L., Miller S.L. (2003) Episodic nutrient transport to Florida coral reefs. *Limnology and Oceanography*, **48**, 1394–1407.

Leichter J.J., Deane G., Stokes M.D. (2005) Spatial and temporal variability of internal wave forcing on a coral reef. *Journal of Physical Oceanography*, **35**, 1945–1962.

Leichter J.J., Payton A., Wankel S., Hanson K., Miller S. (2007) Nitrogen and oxygen isotopic signatures of subsurface nitrate: evidence of deep water nutrient sources to the Florida Keys reef tract. *Limnology and Oceanography*, **52**, 1258–1267.

Leichter J.J., Stokes M.D., Genovese S.J. (2008) Deep water macroalgae seaward of the Florida Keys, USA. *Marine Ecology Progress Series*, **356**, 123–128.

Lloyd M.R. (1964) Variations in the oxygen and carbon isotope ratios for Florida Bay mollusks and their environmental significance. *Journal of Geology*, **72**, 84–111.

McClelland J.W., Valiela I. (1998) Linking nitrogen in estuarine producers to land-derived sources. *Limnology and Oceanography*, **43**, 577–585.

Monismith S., Davis K., Shellenbarger G., Hench J., Nidzieko N., Santoro A., Reidenbach M., Rosman J., Holtzman R., Martens C., Lindquist N., Southwell M., Genin A. (2010) Flow effects on benthic grazing on phytoplankton by a Caribbean reef. *Limnology and Oceanography*, **55**, 1881–1892.

Monseurd R., Leemans R. (1992) Comparing global vegetation maps with the Kappa statistic. *Ecological Modelling*, **62**, 275–293.

Niiler P. (1968) On the internal tidal motions in the Florida Straits. *Deep Sea Research*, **15**, 113–123.

Paytan A., Shellenberger G., Street G.E.M., Gonneea M.E., Davis K., Young B.M., Moore W.S. (2006) Submarine groundwater discharge: an important source of new

nutrients to coral reef ecosystems. *Limnology and Oceanography*, **51**, 343–348.

Pontius R. (2000) Quantification error *versus* location error in comparison of categorical maps. *Photogrammetric Engineering and Remote Sensing*, **66**, 1011–1016.

Raven J., Beardall J., Griffiths H. (1982) Inorganic C-source for *Lemana*, *Cladophora* and *Ranunculus* in a fast-flowing stream: measurement of gas exchange and carbon isotope ratio and their ecological implications. *Oecologia*, **53**, 68–78.

Ren L., Linsley B.K., Wellington G.M., Schrag D.P., Hoegh-Guldberg O. (2002) Deconvolving the δ^{18}O seawater component from subseasonal coral δ^{18}O and Sr/Ca at Rarotonga in the southwestern subtropical Pacific for the period 1726 to 1997. *Geochimica et Cosmochimica Acta*, **67**, 1609–1621.

Rose K., Roth B., Smith E. (2009) Skill assessment of spatial maps for oceanographic modelling. *Journal of Marine Systems*, **70**, 34–48.

Saino T., Hattori A. (1980) N-15 natural abundance in oceanic suspended particulate matter. *Nature*, **283**, 752–754.

Schmidt G.A., Bigg G.R., Rohling E.J. (1999) Global seawater oxygen-18 database – v1.20. http://data.giss.nasa.gov/o18data/ (accessed 10 December 2010).

Smith J.E., Smith C.M., Vroom P.S., Beach K.L., Miller S. (2004) Nutrient and growth dynamics of *Halimeda tuna* on Conch Reef, Florida Keys: possible influence of internal tides on nutrient status and physiology. *Limnology and Oceanography*, **49**, 1923–1936.

Southwell M.W., Popp B.N., Martens C.S. (2008) Nitrification controls on fluxes and isotopic composition of nitrate from Florida Keys sponges. *Marine Chemistry*, **108**, 96–108.

Swart P.K., Healy G.F., Dodge R.E., Kramer P., Hudson J.H., Halley R.B., Robble M.B. (1996) The stable oxygen and carbon isotopic record from a coral growing in Florida Bay: a 160 year record of climatic and anthropogenic influence. *Palaeogeology, Palaeoclimate and Palaeoecology*, **123**, 219–237.

Swart P.K., Lamb K., Saeid A. (2005) Temporal and spatial variation in the δ^{15}N and δ^{13}C of coral tissue and zooxanthellae in *Montastraea faveolata* collected from the Florida reef tract. *Limnology and Oceanography*, **50**, 1049–1058.

Tabouret H., Bareille G., Claverie F., Pecheyran C., Prouzet P., Donard O.X.F. (2010) Simultaneous use of strontium:calcium and barium:calcium ratios in otoliths as markers of habitat: application to the European eel (*Anguilla anguilla*) in the Adour basin, south west France. *Marine Environment Research*, **70**, 35–45.

Umezawa Y., Miyajima T., Yamamuro M., Kayanne J., Koike I. (2002) Fine-scale mapping of land-derived nitrogen in coral reefs by δ^{15}N in macroalgae. *Limnology and Oceanography*, **47**, 1405–1416.

Visser H., De Nijs T. (2006) The map comparison kit. *Environmental Modelling and Software*, **21**, 346–358.

Vroom P.S., Smith C.M., Coyer J.A., Walter L.J., Hunter C.L., Beach K.S., Smith J.E. (2003) Field biology of *Halimeda tuna* (Bryopsidales, Chlorophyta) across a depth gradient: comparative growth, survivorship, recruitment, and reproduction. *Hydrobiologia*, **501**, 149–166.

Ward-Paige C.A., Risk M.J., Sherwood O.A. (2005) Reconstruction of nitrogen sources on coral reefs: δ^{15}N and δ^{13}C in gorgonians from the Florida Reef Tract. *Marine Ecology Progress Series*, **296**, 155–163.